JACS
JOURNAL OF THE AMERICAN CHEMICAL SOCIETY
Communication
Cite This: J. Am. Chem. Soc. 2017, 139, 15584-15587
pubs.acs.org/JACS

# Visible-Light-Driven Valorization of Biomass Intermediates Integrated with $H_2$ Production Catalyzed by Ultrathin Ni/CdS Nanosheets

Guanqun Han,[†] Yan-Huan Jin,[‡] R. Alan Burgess,[†] Nicholas E. Dickenson,[†] Xiao-Ming Cao,*[,‡] and Yujie Sun*[,†]

[†]Department of Chemistry and Biochemistry, Utah State University, Logan, Utah 84322, United States

[‡]Centre for Computational Chemistry and Research Institute of Industrial Catalysis, School of Chemistry and Molecular Engineering, East China University of Science and Technology, Shanghai 200237, China

Supporting Information

**ABSTRACT:** Photocatalytic upgrading of crucial biomass-derived intermediate chemicals (i.e., furfural alcohol, 5-hydroxymethylfurfural (HMF)) to value-added products (aldehydes and acids) was carried out on ultrathin CdS nanosheets (thickness ~1 nm) decorated with nickel (Ni/CdS). More importantly, simultaneous $H_2$ production was realized upon visible light irradiation under ambient conditions utilizing these biomass intermediates as proton sources. The remarkable difference in the rates of transformation of furfural alcohol and HMF to their corresponding aldehydes in neutral water was observed and investigated. Aided by theoretical computation, it was rationalized that the slightly stronger binding affinity of the aldehyde group in HMF to Ni/CdS resulted in the lower transformation of HMF to 2,5-diformylfuran compared to that of furfural alcohol to furfural. Nevertheless, photocatalytic oxidation of furfural alcohol and HMF under alkaline conditions led to complete transformation to the respective carboxylates with concomitant production of $H_2$.

Green generation of hydrogen ($H_2$) has attracted increasing attention, in that $H_2$ is not only a clean fuel but also an important commodity chemical.[1] Solar-driven $H_2$ production via semiconductor/co-catalyst systems is generally regarded as a promising approach in transforming and storing intermittent solar energy in chemical forms (i.e., $H_2$).[2] Upon light irradiation, semiconductors will generate excited electrons for proton reduction to yield $H_2$; however, the resultant excited holes will compete to recombine with the excited electrons, leading to lower $H_2$ yield. To minimize the recombination of excited electrons and holes, a common strategy is to employ sacrificial electron donors as hole scavengers.[3] However, such a strategy wastes the oxidizing power of the excited holes. Hence, it is desirable to utilize these otherwise-wasted excited holes to drive useful organic transformations, which will boost $H_2$ production and simultaneously yield value-added organic products.

On the other hand, mankind's sustainable development not only requires the capture and conversion of renewable energies (i.e., solar and wind) but also necessitates the production of chemical goods from renewable carbon sources.[4] To decrease our reliance on fossil resources, in addition to renewable energy production, it is equally important to explore renewable carbon sources. In this regard, biomass is the only candidate for sustainable carbon sources, because it stores the contemporary carbon and its consumption does not alter the current carbon balance of our ecosystem.[5] Upon initial treatment of raw biomass materials, there are a large number of biomass-derived intermediate compounds which require further refining to become high-value products.[6] Our group recently reported that electrocatalytic oxidation of biomass-derived intermediates (furfural alcohol, 5-hydroxymethylfurfural (HMF), etc.) could be integrated with electrocatalytic $H_2$ production in aqueous media to produce two types of products simultaneously: upgraded bioproducts on anode and $H_2$ on cathode.[7] To minimize the competing water oxidation reaction, strong alkaline conditions were employed, and only carboxylates were obtained.[7] It remains challenging to achieve the selective oxidation of those biomass-derived intermediates to their corresponding aldehydes via electrocatalysis under alkaline condition because of the Cannizzaro mechanism. Nevertheless, aldehydes (i.e., 2,5-diformylfuran (DFF) from HMF oxidation) are important chemical feedstocks in industry.[8] Conventional approaches in transforming furfural alcohol and HMF to their corresponding aldehydes (furfural and DFF, respectively) typically require high temperature, toxic chemical oxidants, and/or expensive catalysts.[9] Thus, it is necessary to explore alternative greener strategies to upgrade those biomass-derived compounds to more valuable aldehydes and preferably generate $H_2$ simultaneously under milder conditions. Within this context, photocatalysis stands out as an attractive option, and heterogeneous semiconductor/co-catalyst systems represent a promising photocatalysis platform because of their tunable optical properties and facile modification with various functional components.[10]

Here we report that ultrathin CdS nanosheets loaded with co-catalyst Ni (Ni/CdS) are able to transform the aforementioned biomass-derived compounds to aldehydes effectively in neutral water upon visible light irradiation, with concomitant formation of $H_2$. The difference observed for the photocatalytic oxidation of furfural alcohol and HMF in neutral water was probed

Received: August 15, 2017
Published: October 11, 2017





DOI: 10.1021/jacs.7b08657
J. Am. Chem. Soc. 2017, 139, 15584−15587

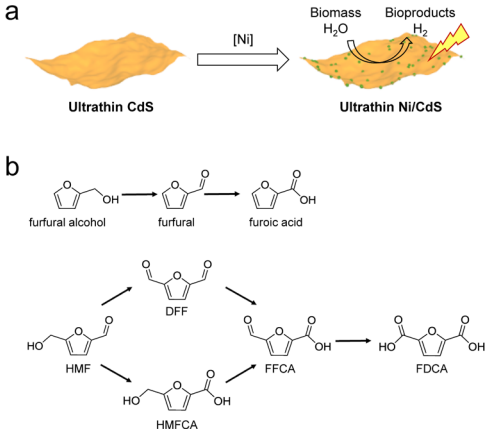


**Figure 1.** (a) Synthetic route of ultrathin Ni/CdS nanosheets for integrated $H_2$ production and biomass valorization. (b) Oxidation reactions of furfural alcohol and HMF to their corresponding aldehydes and acids.

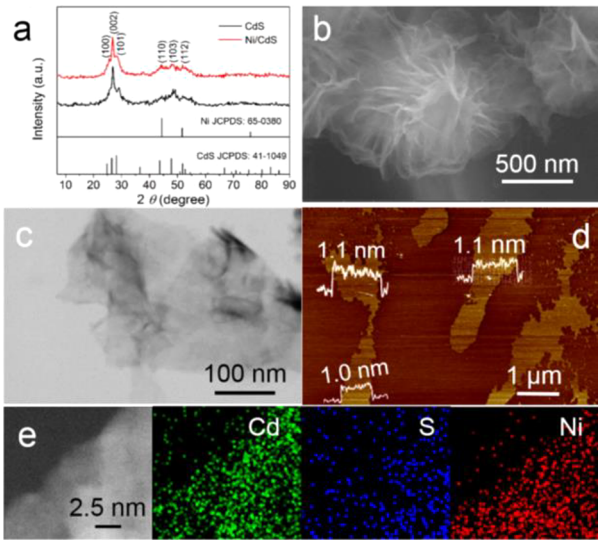


**Figure 2.** (a) XRD, (b) SEM, (c) STEM, (d) AFM, and (e) elemental mapping images of Ni/CdS.

experimentally and theoretically. Control experiments and density functional theory (DFT) calculations concluded that the slightly stronger binding affinity of the aldehyde group relative to the alcohol group in HMF toward Ni/CdS influences the oxidation of the latter. Nevertheless, under alkaline conditions, both furfural alcohol and HMF were quickly transformed to their corresponding acids with nearly 100% yields after neutralization. Regardless of reaction conditions, our ultrathin Ni/CdS nanosheets exhibited excellent activity and robust stability. Tuning the catalyst and reaction conditions enables us to achieve either aldehydes or acids selectively as the desirable products, which represents a remarkable advantage compared to our reported electrocatalysis strategy.

Even though CdS has been frequently reported for photocatalysis applications, ultrathin CdS nanosheets (thickness ~1 nm) supported with first-row transition metal co-catalysts have been rarely reported.[11] Herein, we demonstrate that facile microwave treatment followed by chemical reduction allows us to obtain ultrathin CdS nanosheets loaded with controllable amount of Ni. Specifically, CdS nanosheets could be synthesized at 80 °C under microwave irradiation for 30 min utilizing common Cd and S precursors (see Figure S2). X-ray diffraction (XRD) measurement of CdS confirmed its desirable wurtzite crystal structure (Figure 1a).[12] The relatively low crystallinity of CdS is due to its nanosheet morphology with very thin thickness as manifested in its SEM and STEM images (Figure 2b,c). Chemical reduction of $NiCl_2$ in the presence of CdS nanosheets formed ultrathin Ni/CdS. Varying the original $NiCl_2$ mass percentage from 5% to 20% did not lead to new apparent Ni-based crystalline peaks (Figures 1a and S3) or alter the nanosheet morphology (Figures S4 and S5), suggesting that either the resultant Ni were amorphous or their sizes were too small to be detected by powder XRD. Elemental analysis via ICP-OES of the above four Ni/CdS samples resulted in the final mass percentage of Ni as 0.64%, 1.40%, 2.66%, and 4.68%, respectively (Table S1). Screening experiments demonstrated that the 2.66% Ni/CdS exhibited the best photocatalytic performance (Table S2); thus all the following experiments were carried out with this photocatalyst, which was noted as Ni/CdS for brevity. It is necessary to emphasize that the loading of Ni did not alter the nanosheet thickness. Indeed, the atomic force microscopy (AFM) image of Ni/CdS confirmed its ultrathin thickness of ~1.1 nm (Figure 2d). TEM elemental mapping analysis further confirmed the even distribution of Ni, Cd, and S within Ni/CdS (Figure 1e), and no Ni aggregate was observed under high magnification. The BET surface areas of CdS and Ni/CdS were measured to be 63 and 64 $m^2/g$, respectively (Figure S6). Metallic Ni species were corroborated by X-ray photoelectron spectroscopy (XPS) results (Figures S7). The high-resolution Ni 2p spectrum could be deconvoluted into two subsets of peaks at 852.4 and 870.0 eV attributed to metallic Ni,[13] and at 858.2 and 876.5 eV assignable to $Ni^{2+}$.[14] The presence of $Ni^{2+}$ is most likely due to formation of nickel oxide/hydroxide when exposed to air during sample handling. The ratio of $Ni^{2+}$ to Ni based on XPS results was calculated to be ~1. Different from reported CdS nanoparticles and nanorods,[15] it was anticipated such an ultrathin two-dimensional morphology of Ni/CdS would facilitate charge migration to the catalyst surface and its overall interaction with reaction substrates.

The photocatalytic performance of Ni/CdS for biomass valorization coupled with $H_2$ production was first assessed with furfural alcohol (10 mM) oxidation in water, using a blue LED (450 nm, 8 W) as the light source. Photoluminescence (Figure S8) and $^1H$ NMR (Figure S9) results using terephthalic acid as the organic substrate demonstrated that there was nearly no $OH^•$ formed during the photocatalysis process (see Supporting Information (SI)). The timeline of generated $H_2$ volume over time during the first 8 h irradiation was plotted in Figure 3a, which showed a rapid increase during the first 2 h and approached a plateau after 8 h. Simultaneously, the organic

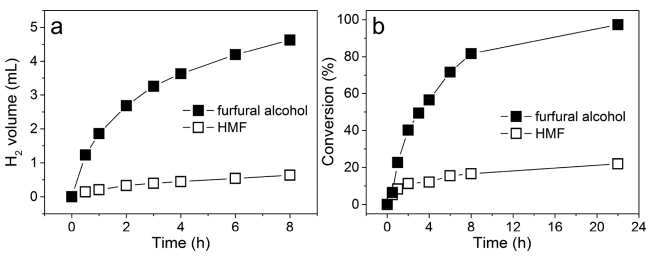


**Figure 3.** (a) Produced $H_2$ volume and (b) conversion of organic substrates during photocatalysis. Conditions: 10 mM organic substrate and 10 mg of Ni/CdS in 10 mL of $H_2O$, blue LED.



DOI: 10.1021/jacs.7b08657
J. Am. Chem. Soc. 2017, 139, 15584−15587

product from furfural alcohol oxidation was identified and quantified by HPLC and $^1$H NMR. Figure 3b displays the conversion change of furfural alcohol over time. After 22 h photocatalysis, nearly 100% conversion of furfural alcohol to furfural was achieved (Figure S10). Besides excellent activity, our Ni/CdS also exhibited robust stability. Recycling the same Ni/CdS catalyst for four consecutive photocatalysis cycles did not show any activity decrease (Figures S11 and S12). Over 90% conversion of furfural alcohol was achieved for all the photocatalysis runs and the selectivity of furfural was almost 100% utilizing the same Ni/CdS photocatalyst. Post-photocatalysis characterization of Ni/CdS indicated its retaining crystallinity, morphology, and elemental distribution (Figures S13–S15).

Such a promising photocatalytic activity of Ni/CdS prompted us to explore another more useful reaction, the oxidation of HMF to DFF, which could not be accomplished using our reported electrocatalysis strategy.[7] Surprisingly, under the same photocatalysis condition (10 mM HMF and 10 mg of Ni/CdS in 10 mL of water), the conversion of HMF to DFF was significantly lower than that of furfural alcohol oxidation (Figures 3b and S16). Only 20% conversion was achieved after 22 h photocatalysis, even though the selectivity of DFF was still close to 100%. Accordingly, the produced $H_2$ yield was also much lower when HMF was employed as the hole scavenger (Figure 3a). Given the oxidation of furfural alcohol and HMF to their corresponding aldehydes involves a very similar hydroxymethyl group, such a disparity in their conversation rates under the same reaction condition strongly implies the influence of the aldehyde group in HMF on the oxidation of its alcohol group.

To explore the role of ancillary substituents in the oxidation of the alcohol group in HMF, we designed two control experiments using 10 mM 2,5-dihydroxymethylfurfural (DHMF) and 5-hydroxymethyl-2-furan-carboxylic acid (HMFCA) as the organic substrates. The oxidation route of DHMF is shown in Figure 4a. As plotted in Figures 4b and S17, the concentration evolution of DHMF and its oxidation products over a 22 h photocatalysis demonstrated the dominant product was HMF (7 mM) with only one of the two alcohol groups in DHMF oxidized to aldehyde. The minor product was DFF (2 mM) with some residual DHMF (1 mM). In contrast, if HMFCA was used as the organic substrate, nearly complete conversion to its oxidized product, 2-formyl-5-furancarboxylic acid (FFCA), was obtained (Figures 4c and S18). Collectively, the results of these control experiments suggest that the presence of an aldehyde group indeed hindered the oxidation of the alcohol group in HMF; however, ancillary alcohol and acid groups do not present any negative impact. Hence, it is likely that the different binding affinities of these substituents toward Ni/CdS may result in the oxidation disparity. Consequently, DFT computations were carried out to shed more light on the binding affinity of aldehyde and alcohol groups in HMF to Ni/CdS.

Since the formed holes after photoexcitation and electron–hole pair separation would most likely migrate to nickel oxides, which were mostly likely responsible for organic oxidation, herein we investigated the adsorption of HMF over the prevalent NiO(001) facets in the presence of aqueous solution utilizing screened hybrid functional HSE06[16] with van der Waals correction implemented in VASP package[17] (see SI). As displayed in Figure 4d, HMF could vertically adsorb atop the Ni site at water/NiO(001) interface via the oxygen atom of its aldehyde group or alcohol group. If the aldehyde group is adsorbed to the NiO(001) surface, its alcohol group would swing

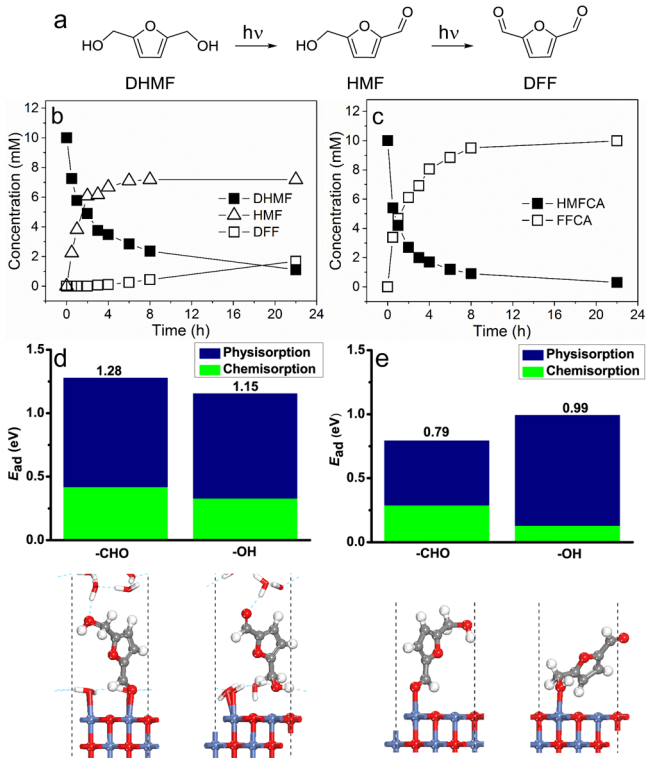


**Figure 4.** (a) Oxidation of DHMF to HMF and DFF. (b,c) Concentration change over time for the photocatalysis of DHMF (b) and HMFCA (c). Conditions: 10 mM organic substrate and 10 mg of Ni/CdS in 10 mL of $H_2O$, blue LED. (d) Adsorption structures and energies of HMF at water/NiO(001) interface via its aldehyde group or alcohol group. (e) Adsorption structures and energies of HMF over bare NiO(001) surface via its aldehyde group or alcohol group.

away from the catalyst surface, and vice versa. It is apparent that the adsorption of HMF via its aldehyde group is 0.13 eV more stable than that via the alcohol group at water/NiO(001) interface, indicating that HMF prefers to adsorb at water/NiO(001) interface via the aldehyde group. As a consequence, the oxidation occurring at alcohol group far away from the NiO(001) surface is unfavorable. In contrast, without considering surface water, HMF prefers to adsorb on NiO(001) via its alcohol group rather than the aldehyde group (Figure 4e). This may be ascribed to the competitive adsorption between water and HMF over NiO(001). The furan ring in HMF would tilt toward NiO(001) when HMF is chemisorbed via alcohol group to enhance its physisorption energy. However, in the presence of aqueous solution, the co-adsorbed water on NiO(001) surface prevents the furan ring from approaching to the NiO(001) surface. Accordingly, the adsorption via aldehyde group with slightly stronger chemisorption is preferred. Thus, we tend to believe that during photocatalysis, HMF is more likely adsorbed on the NiO(001) surface via its aldehyde group while the alcohol group is far away from the catalyst surface, leading to the slower oxidation from HMF to DFF under neutral condition.

Besides neutral water, we also sought to evaluate the performance of Ni/CdS for the oxidation of these biomass-derived intermediates under alkaline condition (Figure 5). Owning to the Cannizzaro mechanism, aldehyde groups are not stable at high pH and will disproportionate to form alcohols and acids.[18] As expected, the concentration profiles of furfural alcohol oxidation in 10 M NaOH showed a rapid decrease of the starting compound and immediate formation of furoic acid within 10 min


DOI: 10.1021/jacs.7b08657
J. Am. Chem. Soc. 2017, 139, 15584–15587

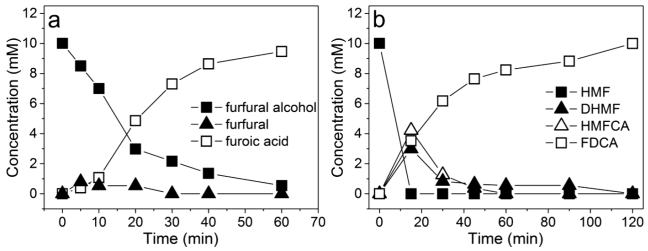


**Figure 5.** Concentration change over time for the photocatalytic oxidation of (a) furfural alcohol and (b) HMF under alkaline conditions (10 mM furfural alcohol and 10 mg of Ni/CdS in 10 mL of 10 M NaOH, blue LED).

under photocatalysis (Figure 5a). Over 90% yield was obtained for the production of furoic acid in only 1 h photocatalysis, much more efficient than the oxidation rate in neutral water. Even though furfural was detected during the whole process, its concentration was remained quite low (<1 mM), in agreement with its weak stability at high pH. Analogous results were obtained for the photo-oxidation of HMF to FDCA with nearly unity HMF conversion and FDCA yield (Figure 5b). Post-photocatalysis characterization of Ni/CdS via SEM and elemental mapping demonstrated its excellent stability under strongly alkaline conditions, and no morphology change and/or aggregation was detected (Figures S19 and S20). Thus, carboxylates also could be obtained via photocatalysis, representing a greener approach complementary to our reported electrocatalysis strategy.

In conclusion, we demonstrated that it is feasible to produce value-added bioproducts (i.e., furoic acid, DFF, and FDCA) and $H_2$ from biomass-derived intermediate compounds in aqueous media, utilizing both excited electrons and holes generated by ultrathin 2D Ni/CdS nanosheets under visible light irradiation. Our work also elucidated the impact of ancillary aldehyde groups in the oxidation of the hydroxymethyl group in HMF. Overall, this photocatalysis strategy enables us to produce aldehydes in neutral water, which was not obtained in our previous electrolysis. In addition, under strong alkaline conditions, complete photocatalytic conversion of furfural alcohol and HMF to their corresponding carboxylates was also realized.

## ■ ASSOCIATED CONTENT

### Supporting Information

The Supporting Information is available free of charge on the ACS Publications website at DOI: 10.1021/jacs.7b08657.

Experimental details and characterization data (PDF)

## ■ AUTHOR INFORMATION


### Corresponding Authors

*xmcao@ecust.edu.cn

*yujie.sun@usu.edu

### ORCID

Nicholas E. Dickenson: 0000-0003-1572-6077

Xiao-Ming Cao: 0000-0002-4782-853X

Yujie Sun: 0000-0002-4122-6255


### Notes

The authors declare no competing financial interest.

## ■ ACKNOWLEDGMENTS

Y.S. acknowledges the support of the National Science Foundation (CHE-1653978) and the Microscopy Core Facility at Utah State University. X.-M.C. is thankful for financial support from NSFC (21673072 and 21333003), and Program of Shanghai Subject Chief Scientist (17XD1401400), and computing time support from Special Program for Applied Research on Super Computation of the NSFC-Guangdong Joint Fund (the second phase) under Grant No. U1501501.

## ■ REFERENCES


(1) (a) Shao, Y.; Cheng, Y.; Duan, W.; Wang, W.; Lin, Y.; Wang, Y.; Liu, J. *ACS Catal.* **2015**, *5*, 7288. (b) Setzler, B. P.; Zhuang, Z.; Wittkopf, J. A.; Yan, Y. *Nat. Nanotechnol.* **2016**, *11*, 1020. (c) Vojvodic, A.; Medford, A. J.; Studt, F.; Abild-Pedersen, F.; Khan, T. S.; Bligaard, T.; Nørskov, J. K. *Chem. Phys. Lett.* **2014**, *598*, 108. (d) Shipman, M. A.; Symes, M. D. *Catal. Today* **2017**, *286*, 57.

(2) (a) Chen, X.; Shen, S.; Guo, L.; Mao, S. S. *Chem. Rev.* **2010**, *110*, 6503. (b) Thoi, V. S.; Sun, Y.; Long, J. R.; Chang, C. J. *Chem. Soc. Rev.* **2013**, *42*, 2388. (c) Yan, Y.; Crisp, R. W.; Gu, J.; Chernomordik, B. D.; Pach, G. F.; Marshall, A. R.; Turner, J. A.; Beard, M. C. *Nat. Energy* **2017**, *2*, 17052.

(3) (a) Yan, H.; Yang, J.; Ma, G.; Wu, G.; Zong, X.; Lei, Z.; Shi, J.; Li, C. *J. Catal.* **2009**, *266*, 165. (b) Sun, Y.; Sun, J.; Long, J. R.; Yang, P.; Chang, C. J. *Chem. Sci.* **2013**, *4*, 118. (c) Yin, S.; Han, J.; Zou, Y.; Zhou, T.; Xu, R. *Nanoscale* **2016**, *8*, 14438.

(4) (a) Arakawa, H.; et al. *Chem. Rev.* **2001**, *101*, 953. (b) Filiciotto, L.; Balu, A. M.; Van der Waal, J. C.; Luque, R. *Catal. Today* **2017**, DOI: 10.1016/j.cattod.2017.03.008.

(5) (a) De, S.; Dutta, S.; Saha, B. *Catal. Sci. Technol.* **2016**, *6*, 7364. (b) Fang, R.; Luque, R.; Li, Y. *Green Chem.* **2017**, *19*, 647.

(6) (a) Corma, A.; Iborra, S.; Velty, A. *Chem. Rev.* **2007**, *107*, 2411. (b) Gallezot, P. *ChemSusChem* **2008**, *1*, 734. (c) Besson, M.; Gallezot, P.; Pinel, C. *Chem. Rev.* **2014**, *114*, 1827.

(7) (a) You, B.; Liu, X.; Jiang, N.; Sun, Y. *J. Am. Chem. Soc.* **2016**, *138*, 13639. (b) You, B.; Jiang, N.; Liu, X.; Sun, Y. *Angew. Chem., Int. Ed.* **2016**, *55*, 9913. (c) Jiang, N.; You, B.; Boonstra, R.; Terrero Rodriguez, I. M.; Sun, Y. *ACS Energy Lett.* **2016**, *1*, 386. (d) You, B.; Liu, X.; Liu, X.; Sun, Y. *ACS Catal.* **2017**, *7*, 4564.

(8) (a) Rosatella, A. A.; Simeonov, S. P.; Frade, R. F. M.; Afonso, C. A. M. *Green Chem.* **2011**, *13*, 754. (b) Wang, T.; Nolte, M. W.; Shanks, B. H. *Green Chem.* **2014**, *16*, 548.

(9) Punniyamurthy, T.; Velusamy, S.; Iqbal, J. *Chem. Rev.* **2005**, *105*, 2329.

(10) (a) Colmenares, J. C.; Xu, Y. J. *Heterogeneous Photocatalysis, Fundamentals to Green Applications*; Springer: Berlin/Heidelberg, 2016; pp 249−282. (b) Dukovic, G.; Merkle, M. G.; Nelson, J. H.; Hughes, S. M.; Alivisatos, A. P. *Adv. Mater.* **2008**, *20*, 4306. (c) Nuraje, N.; Asmatulu, R.; Mul, G. *Green Photo-active Nanomaterials: Sustainable Energy and Environmental Remediation*; The Royal Society of Chemistry: London, 2016; pp 168−201. (d) Colmenares, J. C.; Luque, R. *Chem. Soc. Rev.* **2014**, *43*, 765.

(11) (a) Xu, Y.; Zhao, W.; Xu, R.; Shi, Y.; Zhang, B. *Chem. Commun.* **2013**, *49*, 9803. (b) Maiti, P. S.; Houben, L.; Bar-Sadan, M. *J. Phys. Chem. C* **2015**, *119*, 10734.

(12) Chen, J.; Wu, X.-J.; Yin, L.; Li, B.; Hong, X.; Fan, Z.; Chen, B.; Xue, C.; Zhang, H. *Angew. Chem., Int. Ed.* **2015**, *54*, 1210.

(13) You, B.; Jiang, N.; Sheng, M.; Bhushan, M. W.; Sun, Y. *ACS Catal.* **2016**, *6*, 714.

(14) You, B.; Sun, Y. *Adv. Energy Mater.* **2016**, *6*, 1502333.

(15) (a) Tang, M. L.; Grauer, D. C.; Lassalle-Kaiser, B.; Yachandra, V. K.; Amirav, L.; Long, J. R.; Yano, J.; Alivisatos, A. P. *Angew. Chem., Int. Ed.* **2011**, *50*, 10203. (b) Chai, Z.; Zeng, T.-T.; Li, Q.; Lu, L.-Q.; Xiao, W.-J.; Xu, D. *J. Am. Chem. Soc.* **2016**, *138*, 10128.

(16) Heyd, J.; Scuseria, G. E.; Ernzerhof, M. *J. Chem. Phys.* **2006**, *124*, 219906.

(17) (a) Kresse, G.; Hafner, J. *Phys. Rev. B* **1994**, *49*, 14251. (b) Kresse, G.; Furthmüller, J. *Comput. Mater. Sci.* **1996**, *6*, 15.

(18) Vuyyuru, K. R.; Strasser, P. *Catal. Today* **2012**, *195*, 144.




DOI: 10.1021/jacs.7b08657
J. Am. Chem. Soc. 2017, 139, 15584−15587